



NEW ZEALAND SOCIETY FOR EARTHQUAKE ENGINEERING

## 2019 Pacific Conference on Earthquake Engineering

TURNING HAZARD AWARENESS INTO RISK MITIGATION

4 – 6 April | SkyCity, Auckland | New Zealand



---

# A robust procedure for analysis and design of seismic resistant structures with flag-shaped hysteretic damping systems

*A. Hashemi, H. Bagheri, P. Quenneville*

Department of Civil and Environmental Engineering, The University of Auckland, Auckland.

*S.M.M Yousef-Beik, F.M. Darani, P. Zarnani*

Department of Built Environment Engineering, Auckland University of Technology, Auckland.

### ABSTRACT

Different design codes around the world have different approaches to determine the design seismic loads yet most of them recommend reducing the elastic base shear by a factor that is related to the ductility of the structure. Some of the codes recommend values for different types of lateral load resisting system and the material used. Nevertheless, there is lack of information about the seismic design of the structures with more advanced technologies such as flag-shaped damping devices.

While the flag-shaped energy dissipation devices bring superior seismic performance (including the self-centring behaviour) for the structure, lack of a robust and efficient method for designing and sizing these dampers may be a barrier for the decision-makers to adopt this technology. One important reason could be the extra cost resulted from the inefficient sizing of the structure and the devices.

This paper provides a robust step-by-step analysis and design procedure for engineers in practice and researchers for designing a structure with flag-shaped damping systems. This procedure which is based on the Equivalent Static Method (ESM) may require pushover and nonlinear time-history analyses to verify the performance.

A case-study multi-storey structure that uses timber shear walls with Resilient Slip Friction Joint (RSFJ) hold-downs (with flag-shaped hysteresis) is considered to follow and verify the proposed procedure. It is shown that efficient design could result in smaller dampers and less demand in the

*A robust procedure for analysis and design of seismic resistant structures with flag-shaped hysteretic...*

walls. The findings confirm that the proposed approach can be used to efficiently design the structure with flag-shaped hysteretic damping devices.

## 1 INTRODUCTION

The observations after the Canterbury earthquake sequence (2010 to 2012) in New Zealand indicated that many buildings (specially steel structures) performed as expected, however, since the structures were designed for the ‘life-safety’ criteria, post-disaster repair costs (if the structure is repairable) and the associate business downtime have significantly affected the economy of the recovering city (Bruneau & MacRae, 2017). In addition to implementing energy dissipation devices in structures to reduce the earthquake damage, the ability to return to the pre-earthquake state has a significant effect in the post-event functionality of the structures. More to the point, Erochko et al. (2010) asserted that residual drifts more than 0.5% can be considered as the total loss threshold where replacing the building is more economical than repairing it. McCormick (2008) et al. also reported 0.5% as the permissible residual drift ratio based on the post-event functionality criteria.

To compensate for this issue, self-centring structural solutions have been developed by researchers and engineers to encourage the post-event functionality design criteria and minimize the residual displacement. Successful examples of the self-centring systems developed are Self-Centring Energy Dissipative (SCED) steel braces (Tremblay et al., 2008), the PREcast Seismic Structural System (PRESSS) (Priestley et al., 1999) and Pres-Lam system for timber structures (Sarti et al., 2015).

The innovative Resilient Slip Friction Joint (RSFJ) has recently been developed and introduced to the New Zealand construction industry (Zarnani & Quenneville, 2015). The device that already has been implemented in two real projects (and is under study for more), provides self-centring behaviour and seismic energy dissipation with a flag-shaped hysteresis. It also includes a built-in collapse prevention secondary fuse function that adds more resiliency to the system in case of a seismic event larger than the design level. Hashemi et al. (2018) experimentally verified the flag-shaped hysteresis and the self-centring characteristic of the RSFJ.

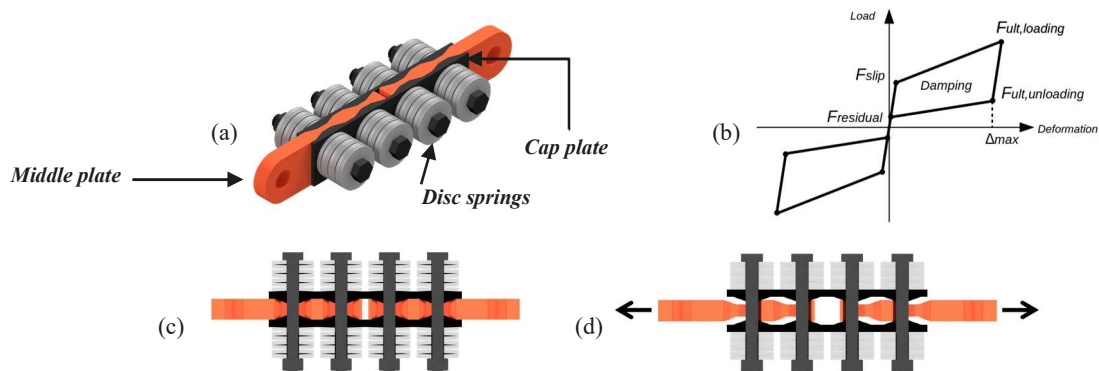


Figure 1: Resilient Slip Friction Joint (RSFJ): (a) assembly, (b) hysteresis, (c) the joint at rest, (d) the joint at the maximum deflection

Figure 1 shows the components and the assembly of the RSFJ. In this joint, energy is dissipated by the frictional sliding of the middle moving plates while the specific shape of the ridges combined with the use of disc springs provide the necessary self-centring behaviour. Figure 1(c) shows the device at rest when the disc springs are partially compacted. When the force applied to the joint overcomes the resistance between the clamped plates, the middle plates start to move, and the cap plates start to expand until the joint reaches the maximum deflection where the disc springs are flattened (see Figure 1(d)).

The flag-shaped response of each device can be specified on demand in a way that almost any target flag-shaped is possible to design. The slip force ( $F_{slip}$ ) and the residual force ( $F_{residual}$ ) in the joint can respectively be determined by Equation (1) and Equation (2) where  $F_{b,pr}$  is the clamping force in the bolts,  $n_b$  is the number

of bolts,  $\theta$  is the angle of the ridges,  $\mu_s$  is the static coefficient of friction and  $\mu_k$  is the kinetic coefficient of friction. The ultimate force in loading ( $F_{ult,loading}$ ) and unloading ( $F_{ult,unloading}$ ) can be calculated by substituting  $\mu_s$  and  $F_{b,pr}$  in Equation (1) and Equation (2) with  $\mu_k$  and  $F_{b,u}$ , respectively. It should be noted that the initial stiffness of the RSFJ (the stiffness before  $F_{slip}$  in Figure 1(b)) is related to elastic stiffness of the sliding plates and of any other component connected to the RSFJ.

$$F_{slip} = 2n_b F_{b,pr} \left( \frac{\sin \theta + \mu_s \cos \theta}{\cos \theta - \mu_s \sin \theta} \right) \quad (1)$$

$$F_{residual} = 2n_b F_{b,pr} \left( \frac{\sin \theta - \mu_k \cos \theta}{\cos \theta + \mu_k \sin \theta} \right) \quad (2)$$

The reader is referred to (Hashemi, 2017) for more information about the conducted full-scale experimental tests on different applications of the RSFJs including the test results and discussions.

## 2 THE ANALYSIS AND DESIGN PROCEDURE RECOMMENDED FOR STRUCTURES WITH RSFJS

The Equivalent Static Method (ESM) is the most favourable way to calculate the seismic forces worldwide, due to its simplicity and fairly accurate (yet conservative) results. In this method, the earthquake excitations are represented as horizontal static loads applied to story levels in which the amount of loads usually depend on soil type, period of the structure, importance level, location and the type of the lateral load resisting system. When a ductile behaviour is expected from the structure, the calculated elastic seismic loads are reduced by a factor which is related to the level of ductility. In the New Zealand standard for structural design actions (NZS1170.5, 2004), this factor is defined as the “inelastic spectrum scaling factor ( $k_\mu$ )” which is related to the structural ductility factor ( $\mu$ ) and the period of the structure ( $T_1$ ):

$$k_\mu = \mu \quad (3)$$

$$k_\mu = \frac{(\mu-1)T_1}{0.7} + 1 \quad (4)$$

Damage avoidance self-centring systems are usually more sophisticated in design and also pricier compared to the conventional low damage systems that rely on yielding of the designated components to resist earthquakes. Similar to some other advanced damage-avoidance technologies, RSFJ is also quite flexible in terms of the wide range of specifications (target force and displacement) it can offer. Therefore, the need for a robust method or a procedure available for the designers so that they can optimise the specifications of the RSFJs and size the devices is critical.

Following the discussion above, the step-by-step structural analysis and design procedure shown in Figure 2 is developed and recommended to be used when designing seismic resistant structures with RSFJs. The overall aim of the procedure is to follow the “equivalent ductility” approach and determine the optimum force/displacement capacity of the RSFJs based on a given structural performance and accordingly size the devices. This procedure which is based on the ESM, requires non-linear static push-over simulations to tune the RSFJs and non-linear dynamic time-history simulations to verify the target performance. This procedure generally is compatible with most of the international building standards.

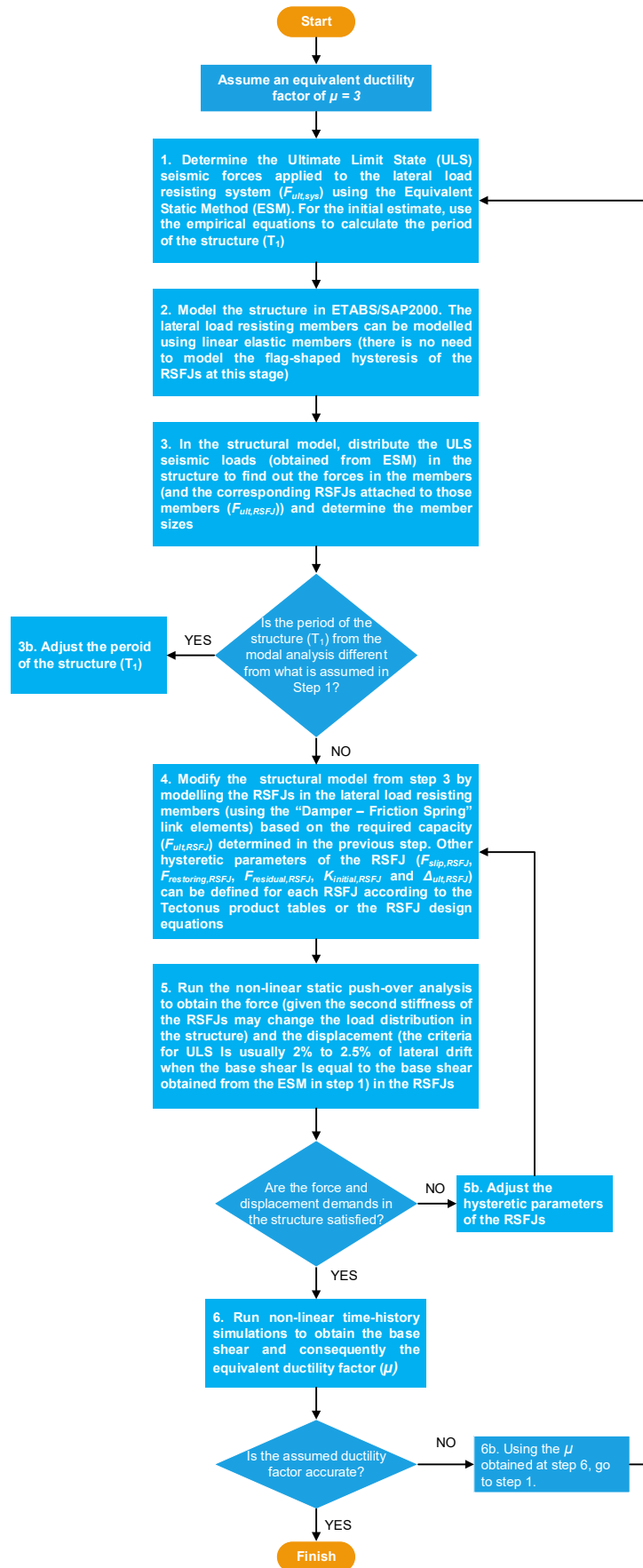


Figure 2: Proposed analysis and design procedure

A robust procedure for analysis and design of seismic resistant structures with flag-shaped hysteretic...

As shown in Figure 2, an equivalent ductility factor of  $\mu = 3.0$  is adopted (a starting point based on the previous parametric studies) at the start and will be verified and optimized by the time-history analysis at the end. When adopting this procedure, iterations may be required to achieve the optimised “equivalent ductility”. Note that as part of the procedure, a model for the structure is required to be developed including the devices. The next section describes each step of the procedure outlined in Figure 2 together with an example case where the procedure is used to design the RSFJs for a structure with timber shear walls.

### 3 NUMERICAL MODELLING OF A FIVE-STORY STRUCTURE WITH RSFJ BRACES

A design example case study building is considered to follow the proposed analysis and design procedure. The considered prototype building is a five-story structure that uses Cross Laminated Timber (CLT) floors, CLT load-bearing walls as the gravity loads resisting members and balloon type CLT shear walls with RSFJ hold-downs at the bottom corners as the lateral load resisting system. Different solutions can be considered for connecting the RSFJs to the CLT walls. Note that since the seismic performance of the system is provided by the geometrically non-linear behaviour of the RSFJs and rest of the structure remains elastic, the performance of the system is independent from the material used for the main structural members. The only concern is how to attach the RSFJs to the structural members which for this case, as shown in (Hashemi, 2017a), long self-tapping screws or bolted connections can be used. It was assumed that the floors and the CLT walls are 200 mm thick panels with five layers of MSG8 timber. The load-bearing CLT panels were assumed to be 150 mm thick with three layers.

The building was designed for soil type C in Christchurch, New Zealand. The total height of the structure is 15 m with 5 m wide spans. Figure 3(a) shows the typical plan view of the structure where each wall uses two RSFJs at the base level. The design permanent loads including the CLT panels, services, ceiling, cladding and self-weight of the structure were specified as 3 kPa and 1.6 kPa for the first four floors and the roof, respectively. The design imposed loads were assumed 2.0 kPa and 0.5 kPa for the first four floors and the roof, respectively. The abovementioned design loads correspond to seismic masses of 190 tonnes and 100 tonnes for the first four floors the roof, respectively. It was decided that the lateral drift ratio of the structure needs to be kept under 1.5%. Note that in this procedure, this limit plays a key role in specifying the maximum design displacement of the RSFJs ( $\Delta_{max}$  in Figure 1(b)) and size the dampers.

The step-by-step flowchart procedure provided in Figure 2 is followed here:

*-Assume an equivalent ductility factor of  $\mu = 3.0$ .*

1. Determine the design seismic forces applied to the lateral load resisting system ( $F_{ult,sys}$ ) using the Equivalent Static Method (ESM). For the initial estimate, use the empirical equations to calculate the period of the structure ( $T_1$ ):

Note that the assumed equivalent ductility factor in this step is the designer’s first assumption. The procedure is designed to verify this assumption and the ultimate goal is that the RSFJs are sized appropriately and the system satisfies the ductility requirement. The structural performance factor ( $S_p$ ) is considered as 0.7. Note that the P-Delta effect is not considered for this example but for a more detailed design in real cases, it must properly be taken into account.

2. Develop a numerical model for the structure. The lateral load resisting members can be modelled using linear elastic members (there is no need to model the flag-shaped hysteresis of the RSFJs at this stage):

The structure is modelled in SAP2000 version 19.0 (CSI., 2017) . Figure 3(b) shows the general arrangement of the numerical model at this stage.

3. In the structural model, distribute the design seismic loads (obtained from ESM) in the structure to find out the forces in the members (and the corresponding RSFJs attached to those members ( $F_{ult,RSFJ}$ ):

*A robust procedure for analysis and design of seismic resistant structures with flag-shaped hysteretic...*

- Is the period of the structure ( $T_1$ ) from the modal analysis different from what is assumed in Step 1?

The period of the structure ( $T_1$ ) at this stage is determined as 0.56 seconds from the modal analysis which is higher than what was assumed in step 1. Therefore, steps 1 to 3 are repeated with this new value. Following the ESM with the new period, the base shear of the structure is reduced from 1150 kN to 956 kN. Then, the force demand in the RSFJs at this stage is 1160 kN. The lever arm for the RSFJ hold-down is assumed as 4.8 m given the width of the RSFJ devices is considered as 200 mm.

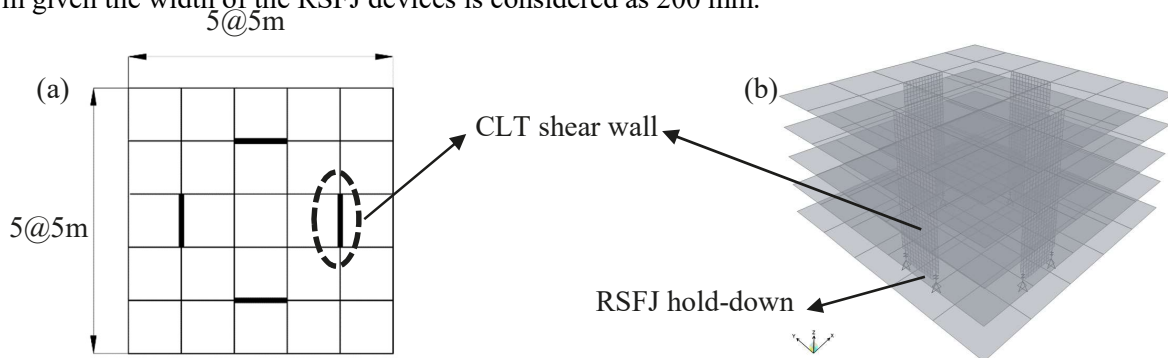


Figure 3: Numerical model of the structure: (a) plan view of the structure, (b) general arrangement

4. Modify the structural model from step 3 by modelling the RSFJs in the lateral load resisting members based on the required capacity ( $F_{ult,RSFJ}$ ) determined in the previous step. Other hysteretic parameters of the RSFJs ( $F_{slip,RSFJ}$ ,  $F_{restoring,RSFJ}$ ,  $F_{residual,RSFJ}$ ,  $K_{initial,RSFJ}$  and  $\Delta_{ult,RSFJ}$ ) can be defined for each RSFJ according to the manufacturer's product tables or from the RSFJ design equations

At this stage, an elastic drift (the drift of the structure at the slip force of the RSFJs ( $F_{slip,sys}$ ) before they start to open) of 0.2% is assumed for the structure. This is consistent with the previous numerical models developed for CLT shear walls (Hashemi, 2016). Based on this and the target design drift limit (1.5%), the displacement demand of the RSFJ hold-downs was determined as 62 mm. Table 1 shows the specifications for the required RSFJs that are determined with respect to the force demands (specified in the previous step) and the design equations provided in (Hashemi et al., 2017a).

Table 1. Initial configuration of the RSFJ hold-downs

Initial stiffness (kN/mm)	$F_{slip}$ (kN)	$F_{ult,loading}$ (kN)	$F_{ult,unloading}$ (kN)	$F_{residual}$ (kN)	$\Delta_{max}$ (mm)
600	580	1160	435	235	62

Following step 4, the RSFJs were modelled using the “Damper – Friction Spring” link element (available in SAP2000 and ETABS). The accuracy of using this link element for numerical modelling of the RSFJs have previously been verified by comparing the experimental data with numerical results (Hashemi, 2017). For each RSFJ, the numerical parameters of the corresponded link element were calibrated using the definitions described in (Hashemi, 2017b).

5. Run the non-linear static pushover analysis to obtain the force and the displacement in the RSFJs.

The results of the non-linear static pushover analysis are displayed in Figure 4. The structure is pushed to 1.5% of lateral drift corresponding to 225 mm of deflection at the roof. Please note that the terminology “non-linear static pushover analysis” is used here but the non-linearity is in fact provided by the non-linear geometrical

*A robust procedure for analysis and design of seismic resistant structures with flag-shaped hysteretic...*

behaviour of the RSFJs. All structural components up to the design drift (1.5%) still behave within their elastic limit. This step ensures that the RSFJs are properly sized to satisfy the force/displacement demands assumed for the design.

- Are the force and displacement demands in the structure satisfied?

It can be seen in Figure 4 that the maximum force in the system at the given drift (1.5%) is 948 kN which is consistent with the base shear from the ESM (956 kN).

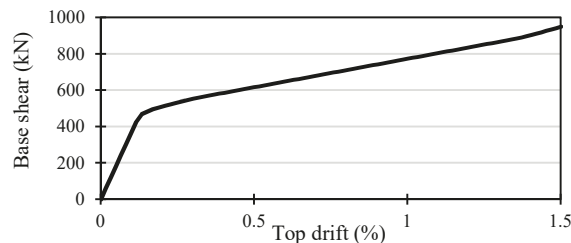


Figure 4: Results of the first non-linear static pushover analysis

6. Run non-linear time-history simulations to obtain the base shear and consequently the equivalent ductility factor ( $\mu$ )

Non-linear dynamic time-history simulations were carried out to investigate the behaviour of the structure. 10 records were chosen for the analysis (PEER, 2015) which were scaled based on the New Zealand standard for the design level (with 1/500 probability of exceedance) for the given soil type and location.

Figure 5 shows the maximum base shears recorded during the time-history simulations. As can be seen, the average is 840 kN. Furthermore, the results showed that the average top roof drift was 1.28% that is lower than the target drift (1.5%). Thus, the new equivalent ductility factor is back calculated as  $\mu = 3.4$  which is using Equation (4) (Note that the period of the structure is less than 0.7 seconds) and the  $k_{\mu}$  derived from the records. Given that this ductility factor is higher than the first assumption in Step 1 ( $\mu = 3.0$ ), the procedure needs to be repeated from the start with the new equivalent ductility factor of  $\mu = 3.4$ . Note that in this study, the average response from 10 ground motions is considered for calculations. However, the majority of the international building standards accepts the results of the time history simulations if ‘the peak of 3’ or ‘the average of seven records (or more)’ is considered (Bradley, 2014). Either way, the approach used should be consistent with the chosen building code.

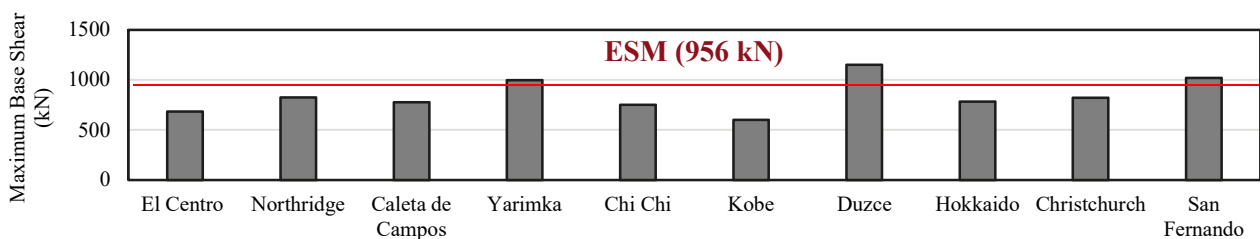


Figure 5: Results of the first Non-Linear dynamic Time-History (NLTH) analysis

This design example shows the efficiency of the proposed procedure and demonstrates that a structural ductility factor as high as 3.4 is achievable for structures when using the RSFJ technology. Nevertheless, it should be noted that the base shear resulted from the ESM tends to be higher than the one from time-history simulations. Therefore, it is in fact the designer’s choice to consider a safety margin between the base shear from the ESM and the base shear from the NLTH simulations before re-sizing the devices. It is recommended that in the last step of the procedure, the base shear from the NLTH is equal or less than the one from the ESM. In this

*A robust procedure for analysis and design of seismic resistant structures with flag-shaped hysteretic...*

example, this margin is not considered for simplicity and the design is optimised by balancing the base shears from NLTH and ESM.

Following the design procedure in Figure 2 with  $\mu = 3.4$ , the new base shear of the structure is determined as 830 kN. Note that the period of the structure ( $T_1$ ) at this stage is increased to 0.58 seconds from the modal analysis which is close enough to what was considered in the first iteration (0.56 seconds). The force demand in the RSFJs is then reduced to 1020 kN and the specifications are revised accordingly (see Table 2).

*Table 2. Revised configuration of the RSFJ hold-downs*

Initial stiffness (kN/mm)	$F_{slip}$ (kN)	$F_{ult,loading}$ (kN)	$F_{ult,unloading}$ (kN)	$F_{residual}$ (kN)	$\Delta_{max}$ (mm)
500	505	1020	370	200	62

Following step 4, the revised RSFJ hold-downs are modelled in SAP2000 using the “Damper – Friction Spring” link element. Following step 5, the results of the revised non-linear static pushover simulation are displayed in Figure 6. As can be seen, the structure performs as expected by reaching the calculated base-shear at the 1.5% drift.

Following step 6 of the procedure, Non-Linear dynamic Time-History (NLTH) simulations were re-conducted on the system. The new average inter-story drift is increased to 1.47% which is consistent with the target drift (1.5%). Moreover, the new average base shear of the structure is 814 kN which is reasonably close to what was specified following the ESM (830 kN). This shows that the adopted ductility factor in the second iteration ( $\mu = 3.4$ ) is consistent with the reality given that the difference between the calculated base shears is under 2%.

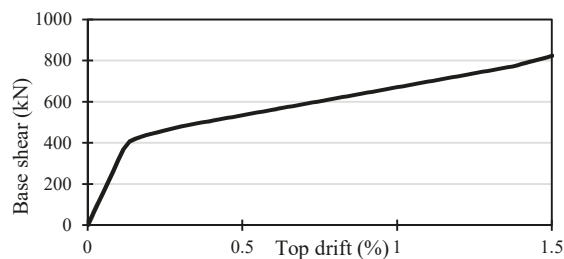


*Figure 5: Results of the revised non-linear static pushover analysis*

#### **4 CALCULATION OF THE SEISMIC FORCES FOR THE PROTOTYPE STRUCTURE USING THE DISPLACEMENT BASED DESIGN (DBD) APPROACH**

A Displacement Based Design (DBD) approach is used in this section to determine the ULS base shear in order to compare the results from the ESM (a Forced Based Design (FBD)) and the DBD for the system. It is shown that by selecting an appropriate hysteresis damping ratio of the structure, both methods can reach to similar conclusions.

Similar to section 2, a design drift ratio limit of 1.5% is considered. According to the DBD approach, the design displacement ( $\Delta_d$ ), the effective mass ( $m_e$ ) and the effective height ( $H_e$ ) can be determined using the following equations:

*A robust procedure for analysis and design of seismic resistant structures with flag-shaped hysteretic...*

$$\Delta_d = \frac{\sum_{i=1}^n m_i \Delta_i^2}{\sum_{i=1}^n m_i \Delta_i} \quad (5)$$

$$m_e = \frac{\sum_{i=1}^n m_i \Delta_i}{\Delta_d} \quad (6)$$

$$H_e = \frac{\sum_{i=1}^n m_i \Delta_i h_i}{\sum_{i=1}^n m_i \Delta_i} \quad (7)$$

It should be noted that the parameters above are specified for the equivalent Single Degree Of Freedom (SDOF) structure representing the prototype building. Table 3 shows the characteristics of the system.

*Table 3. Characteristics of the prototype structure considered for the DBD*

Storey	Height ( $h_i$ )	Mass ( $m_i$ )	$\Delta_i$	$m_i \Delta_i$	$m_i \Delta_i^2$	$m_i \Delta_i h_i$
5	15	100	0.225	22.5	5.06	338
4	12	190	0.180	32.4	6.16	410
3	9	190	0.135	25.7	3.46	231
2	6	190	0.090	17.1	1.54	103
1	3	190	0.045	8.55	0.38	26
Sum				106.1	16.61	1108

Meters for distances and tonnes for masses

Using Equations (5) to (7) and the information in Table 3, the equivalent SDOF structure has a design displacement of  $\Delta_d = 0.15$  m, an effective mass of  $m_e = 702$  tonnes and an effective height of  $H_e = 10.25$  m. The scale factor applicable to the design displacement spectrum (usually with 5% of elastic damping for steel structures) can be determined by Equation (8) where  $\xi_{eq}$  is the equivalent viscous damping ratio of the structure including the elastic and hysteretic damping.

$$R_{eq} = \left( \frac{7}{2 + \xi_{eq}} \right)^{0.5} \quad (8)$$

Assuming a hysteretic damping ratio of 9.5% for the structure (will be verified later),  $R_{eq} = 0.72$  is found. From the scaled displacement spectrum, the effective period of  $T_e = 2.25$  seconds is found for the equivalent SDOF structure. The equivalent lateral stiffness and the base shear can be calculated using Equation (9) and Equation (10).

$$K_e = \frac{T^2}{4\pi^2} S_a \quad (9)$$

$$V_b = K_e \Delta_d \quad (10)$$

For the prototype structure, the effective stiffness and the base shear are determined as  $K_e = 5472$  kN/m and  $V_b = 841$  kN.

It can be seen that the base shears calculated from a FDB (ESM) and the DBD approach are relatively close. (the difference is less than 2%). This means that both approaches can be confidently used when designing a building with RSFJs. However, relatively less effort is required when using the DBD approach. This is because DBD has the advantage of directly incorporating the system damping ratio. The assumed hysteretic damping ratio (9.5%) needs to be verified at this stage. Figure 6 shows the results of the cyclic pushover analysis. The hysteretic damping ratio of the structure can be determined using Equation (11) (Mazza & Vulcano, 2014):

*A robust procedure for analysis and design of seismic resistant structures with flag-shaped hysteretic...*

$$\xi_{hyst} = \frac{2 A_1}{\pi A_2} \quad (11)$$

where  $A_1$  is the area enclosed within the hysteretic loop and  $A_2$  is the area restricted by the elastic-perfectly-plastic loop.

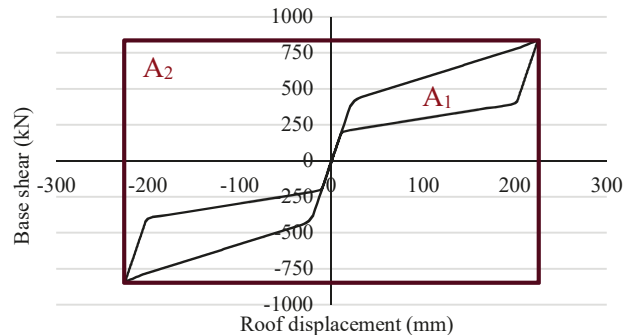


Figure 6. Cyclic pushover analysis

The hysteretic damping ratio calculated by Equation (11) is  $\xi_{hyst} = 9.5\%$  which is consistent with the ratio assumed at the start. Note that iterations maybe required to converge the assumed hysteretic damping ratio at the beginning of the DBD calculations and the one determined from Equation (11) at the end. It is worth mentioning that the flag-shaped response displayed in Figure 6 originates from the RSFJs in the structure. If required by the design, the specifications of the RSFJ ( $F_{slip}/F_{ult,loading}$  proportion and/or the angle of the grooves) can be configured to achieve a higher hysteretic damping ratio.

## 5 CONCLUSIONS

The Resilient Slip Friction Joint (RSFJ) technology is a novel seismic energy dissipation system that has recently been introduced to the construction industry. These joints not only provides energy damping but also a fully self-centring behaviour meaning that the structure will return to its initial position at the end of the seismic event.

This paper provides a step-by-step analysis and design procedure for the structures that uses RSFJs in their lateral load resisting system. This procedure which is based on the Equivalent Static Method (ESM) involves modelling of the structure, performing non-linear static pushover analysis and non-linear dynamic time-history simulations. The proposed design procedure was implemented for a five-story structure with shear walls equipped with RSFJ hold-downs. The findings of this study showed that an equivalent ductility factor of  $\mu = 3.4$  was achievable for the example case study structure. Furthermore, the base shear for the same structure was calculated using a Displacement Based Design (DBD) approach. It was proven that by properly specifying the hysteretic damping ratio of the structure, both methods can reach the same conclusions.

Overall, the findings of this investigation showed that the proposed analysis and design procedure could be efficiently used when RSFJs are employed in seismic resilient structures. Respecting the fact that the ESM and NLTH are internationally recognised and being used, the proposed procedure is compatible to the different international building codes.

## ACKNOWLEDGEMENT

The authors would like to thank Ministry of Business, Innovation and Employment of New Zealand (MBIE) for the financial support of this research.

*A robust procedure for analysis and design of seismic resistant structures with flag-shaped hysteretic...*

## REFERENCES

- Bradley, B. A. (2014). Seismic Performance Criteria Based on Response History Analysis : Alternative Metrics for Practical Application in Nz. *Bulletin of the New Zealand Society for Earthquake Engineering*, 47(3), 1–5.
- Bruneau, M., & MacRae, G. (2017). RECONSTRUCTING CHRISTCHURCH : A Seismic Shift in Building Structural Systems. *Quake Centre Report*.
- Erochko, J., Christopoulos, C., Tremblay, R., & Choi, H. (2010). Residual drift response of SMRFs and BRB frames in steel buildings designed according to ASCE 7-05. *Journal of Structural Engineering*, 137(5), 589–599.
- Hashemi, A. (2017). *Seismic Resilient Multi-story Timber Structures with Passive Damping*. University of Auckland, New Zealand.
- Hashemi, A., Masoudnia, R., & Quenneville, P. (2016). Seismic performance of hybrid self-centring steel-timber rocking core walls with slip friction connections. *Journal of Constructional Steel Research*, 126, 201–213. <http://doi.org/10.1016/j.jcsr.2016.07.022>
- Hashemi, A., Zarnani, P., Masoudnia, R., & Quenneville, P. (2017a). Experimental testing of rocking Cross Laminated Timber (CLT) walls with Resilient Slip Friction (RSF) joints. *Journal of Structural Engineering*, 144(1), 04017180-1 to 04017180-16.
- Hashemi, A., Zarnani, P., Masoudnia, R., & Quenneville, P. (2017b). Seismic resistant rocking coupled walls with innovative Resilient Slip Friction (RSF) joints. *Journal of Constructional Steel Research*, 129, 215–226.
- Hashemi, A., Zarnani, P., Masoudnia, R., & Quenneville, P. (2018). Experimental Testing of Rocking Cross-Laminated Timber Walls with Resilient Slip Friction Joints. *Journal of Structural Engineering (United States)*, 144(1). [http://doi.org/10.1061/\(ASCE\)ST.1943-541X.0001931](http://doi.org/10.1061/(ASCE)ST.1943-541X.0001931)
- Mazza, F., & Vulcano, A. (2014). Equivalent viscous damping for displacement-based seismic design of hysteretic damped braces for retrofitting framed buildings. *Bulletin of Earthquake Engineering*, 12(6), 2797–2819.
- McCormick, J., Aburano, H., Ikenaga, M., & Nakashima, M. (2008). Permissible residual deformation levels for building structures considering both safety and human elements. In *Proceedings of the 14th world conference on earthquake engineering* (pp. 12–17).
- New Zealand Standards. (2004). Structural Design Actions (NZS 1170.5). *Wellington, New Zealand*.
- Nigel Priestley, M. J., Sritharan, S., Conley, J. R., & Pampanin, S. (1999). Preliminary results and conclusions from the PRESSS five-story precast concrete test building. *PCI Journal*, 44(6), 42–67.
- PEER, P. (2015). NGA Database, Pacific Earthquake Engineering Research Center. *University of California, Berkeley, USA*.
- Sarti, F., Palermo, A., & Pampanin, S. (2015). Development and Testing of an Alternative Dissipative Posttensioned Rocking Timber Wall with Boundary Columns. *Journal of Structural Engineering*, E4015011.
- Computers and Structures (2017). SAP2000 Ver. 19 (2017). Berkeley, CA.
- Tremblay, R., Lacerte, M., & Christopoulos, C. (2008). Seismic response of multistory buildings with self-centering energy dissipative steel braces. *Journal of Structural Engineering*, 134(1), 108–120.
- Zarnani, P., & Quenneville, P. (2015). A Resilient Slip Friction Joint. *Patent No. WO2016185432A1*, NZ IP Office.